Z. Phys. C – Particles and Fields 46, 583–591 (1990)

Zeitschrift für Physik C Particles and Fields

$a_2(1320)$ and $\pi_2(1670)$ formation in the reaction $\gamma\gamma \to \pi^+ \pi^- \pi^0$

CELLO Collaboration

H.-J. Behrend, L. Criegee, J.H. Field [1], G. Franke, H. Jung [2], J. Meyer, O. Podobrin, V. Schröder, G.G. Winter
Deutsches Elektronen-Synchrotron, DESY, Hamburg, Federal Republic of Germany

P.J. Bussey, A.J. Campbell, D. Hendry, S. Lumsdon, I.O. Skillicorn
University of Glasgow, Glasgow, UK

J. Ahme, V. Blobel, W. Brehm, M. Feind, H. Fenner, J. Harjes, J.H. Köhne, J.H. Peters, H. Spitzer
II. Institut für Experimentalphysik, Universität, Hamburg, Federal Republic of Germany

W.-D. Apel, J. Engler, G. Flügge [2], D.C. Fries, J. Fuster [3], P. Gabriel, K. Gamerdinger [4], P. Grosse-Wiesmann [5], M. Hahn, U. Hädinger, J. Hansmeyer, H. Küster [6], H. Müller, K.H. Ranitzsch, H. Schneider, R. Seufert
Kernforschungszentrum Karlsruhe und Universität, Karlsruhe, Federal Republic of Germany

W. de Boer, G. Buschhorn, G. Grindhammer [5], B. Gunderson, Ch. Kiesling [7], R. Kotthaus, H. Kroha, D. Lüers, H. Oberlack, P. Schacht, S. Scholz, W. Wiedenmann [8]
Max Planck-Institut für Physik und Astrophysik, München, Federal Republic of Germany

M. Davier, J.F. Grivaz, J. Haissinski, V. Journé, D.W. Kim, F. Le Diberder, J.-J. Veillet
Laboratoire de l'Accélérateur Linéaire, Orsay, France

K. Blohm, R. George, M. Goldberg, O. Hamon, F. Kapusta, L. Poggioli, M. Rivoal
Laboratoire de Physique Nucléaire et des Hautes Energies, Université de Paris, Paris, France

G. d'Agostini, F. Ferrarotto, M. Iacovacci, G. Shooshtari, B. Stella
University of Rome and INFN, Rome, Italy

G. Cozzika, Y. Ducros
Centre d'Etudes Nucléaires, Saclay, France

G. Alexander, A. Beck, G. Bella, J. Grunhaus, A. Klatchko, A. Levy, C. Milstène
Tel Aviv University, Tel Aviv, Israel

Received 10 January 1990

Abstract. The reaction $e^+ e^- \to e^+ e^- \pi^+ \pi^- \pi^0$ in the untagged mode has been measured with the CELLO detector at PETRA. The cross section is dominated by exclusive $a_2(1320)$ production, whose radiative width is determined to be $\Gamma_{\gamma\gamma} = 1.00 \pm 0.07(\text{stat.}) \pm 0.15(\text{syst.})$ keV. An angular correlation analysis indicates pure helicity 2 with an upper limit on the helicity 0 contribution of 8.2% (at 95% c.l.). Excitation of the pseudotensor meson $\pi_2^0(1670)$ is observed for the first time in this reaction. The π_2 radiative width and its dependence on interference effects are studied.

[1] Now at Université de Genève, Switzerland
[2] Now at RWTH, Aachen, Germany
[3] Now at Inst. de Física Corpuscular, Universidad de Valencia, Spain
[4] Now at MPI für Physik und Astrophysik, München, FRG
[5] Now at Stanford Linear Accelerator Center, USA
[6] Now at DESY, Hamburg, Germany
[7] Heisenberg Scholarship of Deutsche Forschungsgemeinschaft
[8] Now at CERN

1 Introduction

The main interest in studying the final state $\pi^+\pi^-\pi^0$ produced in quasi real two photon collisions lies in the measurement of the two photon couplings of $C=+$, isospin 1 resonances. In the quark model, the radiative widths of mesons are proportional to the fourth power of the constituent quark charges and thus provide a sensitive measure of the flavour content. In particular, comparison of the radiative widths of mesons within one J^P nonet can be used as a tool for determining the octet-singlet mixing.

Although the tensor meson $a_2(1320)$ has been observed by many two photon experiments [1–8], its radiative width and especially the helicity structure are still known only with large errors. Recently, the Crystal Ball Collaboration reported preliminary evidence for the formation of the pseudotensor meson $\pi_2^0(1670)$ in the reaction $\gamma\gamma \to 3\pi^0$ [9]. They report consistency with a dominant decay mode $f_2\pi^0$ and a preliminary value for the radiative width of $1.3 \pm 0.3 \pm 0.2$ keV [10].

Since the π_2 is composed of a $q\bar{q}$ pair in an $l=2$ state, quark model predictions are sensitive to the second derivative of the wave function at the origin. A confirmation of the Crystal Ball result is thus of interest. The analysis of π_2 formation in the final state $\pi^+\pi^-\pi^0$ is complicated by the large resonant and non-resonant background from $\rho^\pm\pi^\mp$ and by interference phenomena, which are nearly absent in the $3\pi^0$ final state and completely different from those in the charged π_2 decay, in which branching fractions and phases have been determined [11, 12].

2 Data taking

The experiment was performed with the CELLO detector at the e^+e^- storage ring PETRA at a center of mass energy of 35 GeV. The data correspond to an integrated luminosity of 86 pb^{-1}. Charged tracks are reconstructed in the central detector consisting of nine cylindrical drift chambers and five proportional chambers in a 1.3 T magnetic field provided by a superconducting solenoid, yielding a momentum resolution of $\sigma(p)/p = 0.02 \cdot p$ (p in GeV/c) which can be improved by a vertex constraint. The central detector is surrounded by a fine grained lead-liquid argon calorimeter consisting of 16 barrel and 4 end cap modules. The identification and removal of background due to noise and charged pion reactions in the coil is made possible by means of its good spatial resolution in both the longitudinal and the lateral direction. A detailed description of the CELLO detector is given elsewhere [13].

Low multiplicity untagged $\gamma\gamma$ events were triggered by a fast track-finding processor [14], which basically required two tracks with transverse momentum p_T above 650 MeV/c or two tracks above 250 MeV/c with an opening angle $\Delta\phi$ in the plane perpendicular to the beam larger than 45° (135° for part of the experiment). By applying the same algorithm to the hit pattern of Monte-Carlo events, the trigger decision was reliably simulated.

3 Event selection

To isolate the reaction $e^+e^- \to e^+e^-\pi^+\pi^-\pi^0$, we selected events with two charged tracks with $|\cos\theta| < 0.90$ and one or two isolated electromagnetic showers in the liquid argon calorimeter. In addition to making the usual full π^0 reconstruction through its decay into two photons, we also analyse events with only one observed photon. Monte Carlo studies show that due to the soft photon energy spectrum and our relatively high energy threshold for photon detection ($\varepsilon = 50\%$ at $E = 140$ MeV [15]) a large number of a_2 and π_2 events are expected of the second kind. It is also found that in this event sample invariant masses and decay angular distributions can be reconstructed with only slightly degraded resolution. In an earlier analysis on a smaller data sample [3] we only used this method. In the present analysis, we use both methods in parallel and combine their results at the end. The degree of consistency between the two sets of results serves as a check on the systematic errors. In the following we refer to these datasets as 2γ and 1γ samples, consisting of 7792 and 22043 events, respectively.

The events of both samples are subjected to the following cuts:

- No additional energy deposited in the forward scintillator or the hole tagger.
- Events with photons which could be radiated off one of the charged tracks anywhere along its track through the detector at a small angle ($< 5°$) are likely to be e^+e^- final states and are excluded.
- In order to remove events with photons faked by noise, the transverse momentum of the two charged particles alone should not be balanced. This is achieved by demanding the azimuthal angle $\Delta\phi$ between the two tracks to be less than 175° and the transverse momentum squared of the $\pi^+\pi^-$-system to be larger than 0.03 GeV^2.
- The transverse momentum $p_\perp$ of the whole event including photon(s) should be balanced, with $p_\perp < 0.15$ GeV.

On the remaining events in the 2γ sample we perform a $2C$-fit to zero overall transverse momentum, using a $\sigma(p_\perp)$ of 20 MeV for the unobserved scattered beam electrons. The main effect of this fit is an improvement of the photon energy resolution. The invariant $\gamma\gamma$ mass spectrum of the successfully (probability > 0.01) fitted events is shown in Fig. 1, showing a prominent π^0 signal. We accept the events with invariant $\gamma\gamma$ masses between 80 and 220 MeV as π^0 candidates and perform a second fit on them, imposing $p_\perp$ conservation and the nominal π^0 mass for the $\gamma\gamma$ pair as constraints.

Figure 2a shows the W distribution of the 403 surviving events, dominated by an enhancement around the a_2 mass 1.32 GeV. Figure 3a (with 2 entries per event) demonstrates the dominant presence of intermediate charged ρ resonances in the invariant $\pi^\pm\pi^0$ mass spectrum.

We now proceed to the analysis of the 1γ sample. If the single observed photon provides a good estimate

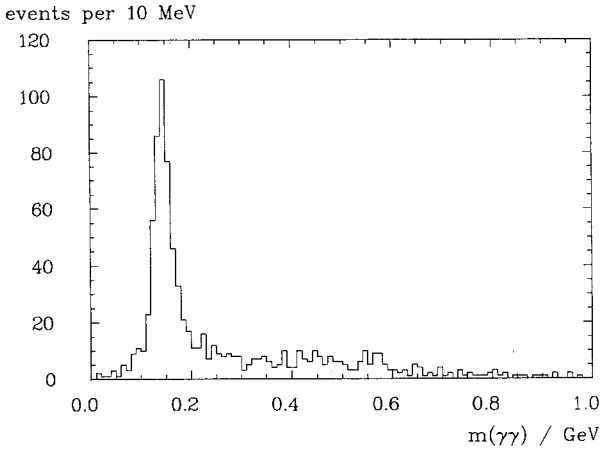

Fig. 1. $m_{\gamma\gamma}$ spectrum in the 2γ sample

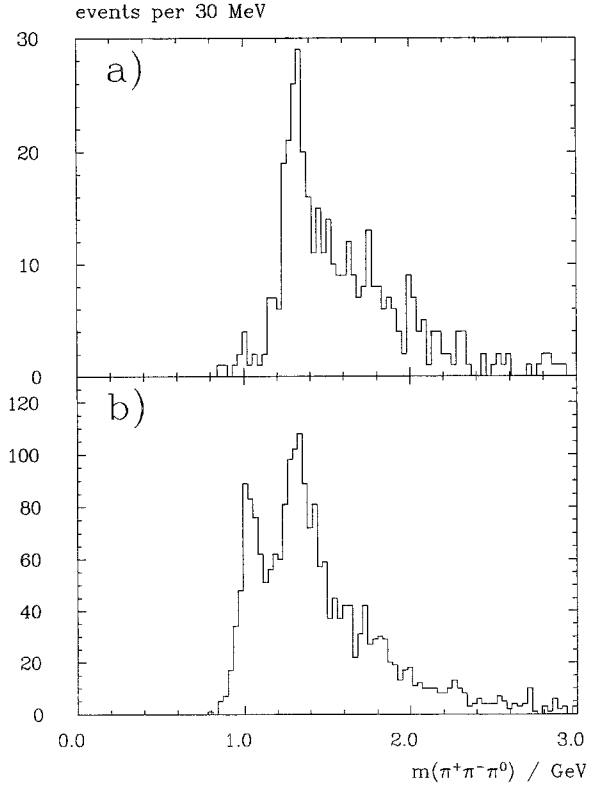

Fig. 2a, b. Invariant $\pi^+\pi^-\pi^0$ mass, **a** 2γ sample, **b** 1γ sample

of the π^0 momentum, it should be able approximately to balance transverse momentum. We thus demand the azimuthal angle between the photon and the $\pi^+\pi^-$ system to lie between 145 and 178°. The upper limit suppresses real $\pi\pi\gamma$ final states (e.g. η' decays), in which no second photon is missing. We furthermore require the measured photon energy to be larger than 150 MeV. The π^0 four vector is then estimated as follows: The direction is simply taken from the observed photon, its momentum is scaled so that the total transverse momentum is minimised (this is approximately achieved for $|\mathbf{p}_\perp(\gamma)| = |\mathbf{p}_\perp(\pi^+\pi^-)|$), and finally the energy is obtained by adding the nominal π^0 mass in quadrature.

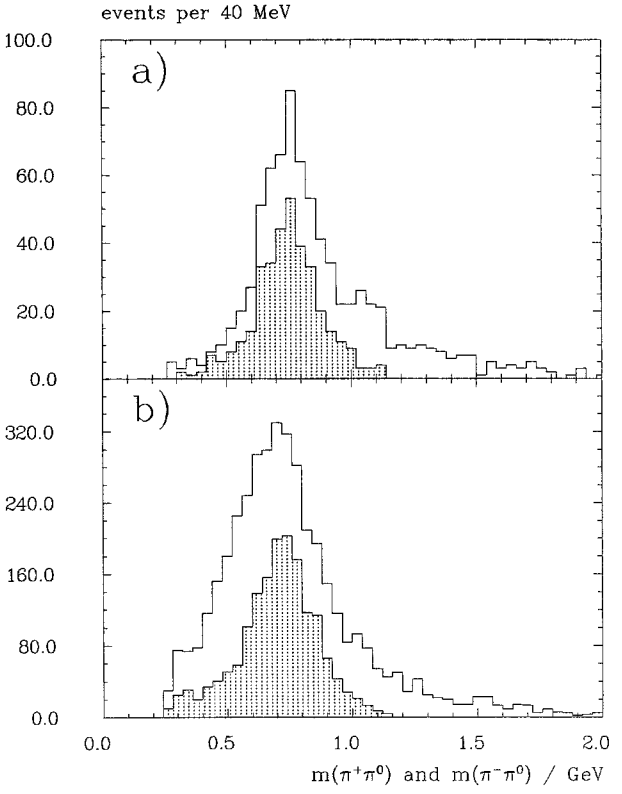

Fig. 3. a $\pi^\pm\pi^0$ mass in 2γ sample, **b** $\pi^\pm\gamma$ mass in 1γ sample. Shaded: $W_{\gamma\gamma}$ restricted to a_2 region

The invariant 3π mass spectrum of these 2154 events is shown in Fig. 2b. Again, a clear $a_2(1320)$ signal is visible. At lower masses one can observe a residual $\eta' \to \pi^+\pi^-\gamma$ signal. The charged 2π combinations are plotted in Fig. 3b, again showing a dominating ρ signal, which is especially prominant if the 3π mass is restricted to the a_2 mass range (shaded area).

In the following we investigate both data samples in terms of resonance formation, analysing the two-photon coupling of the a_2 and also the π_2, which shows up only after further search. We give first a description of the theoretical background and the Monte Carlo simulation.

4 Theoretical preliminaries and Monte Carlo simulation

Since a state formed by two photons has positive charge conjugation and the G-parity of 3 pions is odd, only isospin 1 states are accessible in the reaction $\gamma\gamma \to \pi^+\pi^-\pi^0$. Possible intermediate 2π resonances ("isobars") are the proposed "f_0" in the $\pi^+\pi^-$ s-wave, f_2 in the $\pi^+\pi^-$ d-wave and $\rho^\pm$; the presence of neutral ρ's is forbidden by isospin invariance.

In an untagged $\gamma\gamma$ reaction at an e^+e^- storage ring the cross section can be considered as the sum of three incoherent terms [16]: after integration over azimuthal angles there is no interference between helicity 0 and 2 [17], and after photon helicity summations there is no interference between positive and negative naturality helicity 0 states [16] (the latter argument does not hold

for helicity ± 2). Gauge invariance and Bose symmetry forbid the formation of the spin parity states $J^P = 1^{\pm}, 3^-, 5^-$ etc. as well as any state with helicity 1 by two real photons [18–20]. The same arguments fix the produced helicity to 0 for $0^-, 2^-, 4^-, \ldots$ and to 2 for $3^+, 5^+, 7^+, \ldots$. States with even spin and positive parity can be produced both in helicity 0 and 2. The coupling of a 0^+ state to 3 pions is forbidden by parity. Thus, in the region below 2 GeV, where no resonances with the allowed quantum numbers and $J>2$ are expected, the cross section should be dominated by two incoherent $J^P=2^+$ terms with helicity 2 and 0, and a negative naturality helicity 0 term. The former can contain the $a_2(1320)$, and the latter can be a coherent sum of 0^- with a possible $\pi(1300)$ and $2^-(\pi_2(1670))$.

To extract resonance parameters from the experimental data, a model for production and decay of the resonance R is needed. We use a standard isobar model description for the 3 pion decays, i.e. a coherent sum of the different intermediate resonance amplitudes. Bose symmetry of the complete $R \to 3\pi$ decay amplitude (consisting of an isospin and a spin-parity part) fixes the sign between ρ^+ and ρ^- [16, 21]. For the a_2, this leads to a constructive interference of the ρ-bands on the Dalitz plot [22]. This procedure, though violating three-particle unitarity, has been shown to yield sensible results [23–25].

The $\gamma\gamma \to R \to \pi^+\pi^-\pi^0$ amplitude can be written in a Breit Wigner form:

$$T_{ab} = \frac{M_{ab}\,\delta^{\lambda}_{a-b}\,D_{\lambda}}{m_R^2 - W^2 - i m_R\,\Gamma(W)}, \tag{1}$$

where M_{ab} denote the $\gamma\gamma \to R$ helicity amplitudes as defined by Poppe [20]. However, in the case of tensor meson formation, we take the W-dependence of both helicity 0 and helicity 2 amplitudes to be flat, since Poppe's helicity amplitude definition leads to unitarity violation [26] and at least needs some phenomenological damping term away from threshold [27]; furthermore it cannot be justified from first principles [16].

D_{λ} is the isobar model decay amplitude

$$D_{\lambda} = \sum_I \frac{\Sigma_{\lambda_I} D^{(1)}_{\lambda\lambda_I}(R_{\lambda} \to \pi I_{\lambda_I})\, D^{(2)}_{\lambda_I}(I_{\lambda_1} \to 2\pi)}{m_I^2 - m_{\pi\pi}^2 - i m_I\,\Gamma_I(m_{\pi\pi})} \tag{2}$$

where I denotes the intermediate resonance and λ the helicity*. The $D_I^{(i)}$ are calculated using Born term tensors [21, 20], with coupling constants modified by appropriate Blatt-Weisskopf form factors [29, 30] with $r = 1\,fm$ as a phenomenological description of finite size effects. Whereas the orbital angular momentum settings of the a_2 decay vertices are unique, the $\pi_2 \to f_2\pi$ can decay via $L=0$, 2 and 4, of which only $L=0$ is considered here.

In the limit of real photons the $\gamma\gamma$ cross section can be written as

$$\sigma_{\gamma\gamma \to R \to 3\pi} = \frac{1}{4 W_{\gamma\gamma}^2} \int (|T_{++}|^2 + |T_{+-}|^2)\, d\,\mathrm{Lips}(3\pi) \tag{3}$$

$$= 8\pi(2J_R+1)\frac{m_R^2}{W_{\gamma\gamma}^2} \cdot (\Gamma_{\gamma\gamma}^{(\lambda=0)} + \Gamma_{\gamma\gamma}^{(\lambda=2)}) \cdot \frac{\Gamma(W)\cdot B(R \to \pi I)\cdot B(I \to \pi\pi)}{(m_R^2 - W_{\gamma\gamma}^2)^2 + m_R^2\,\Gamma(W)^2} \tag{4}$$

with J_R being the spin of the resonance R and $\Gamma_{\gamma\gamma} = \Gamma_{\gamma\gamma}^{(0)} + \Gamma_{\gamma\gamma}^{(2)}$ the radiative width with its helicity 0 and helicity 2 contributions. The latter equation follows by applying the golden rule for the decays $R \to 3\pi$ as well as $R \to \gamma\gamma$ [30, 20, 16]:

$$\Gamma(W)\cdot B(R \to \pi I)\cdot B(I \to \pi\pi) = \frac{1}{2 m_R} \int |D_{\lambda}|^2\, d\,\mathrm{Lips}(3\pi) \tag{5}$$

$$\Gamma_{\gamma\gamma}^{(2)} = \frac{1}{16\pi(2J_R+1)\,m_R}\,|M_{+-}|^2;$$

$$\Gamma_{\gamma\gamma}^{(0)} = \frac{1}{16\pi(2J_R+1)\,m_R}\,|M_{++}|^2. \tag{6}$$

For normalisation purposes (5) is also used to calculate the relevant coupling constants needed for the D_{λ} with the PDG [12] values for masses, partial and total widths as input (the result is independent of λ). Note that in this calculation interference has to be taken into account, which is as large as 20% for the a_2 [31]. The case of the π_2 is more complicated because of the presence of many isobars: there is experimental evidence for $f_2\pi^0$ (S and D wave), $\rho^{\pm}\pi^{\mp}$, and $(\pi^+\pi^-)_{s\text{-wave}}\,\pi^0$ [12]. The decay Dalitz plot and angular distributions of the π_2 not only depend on the branching ratios, but also on the relative phases between these intermediate state amplitudes. Since they refer to different J^P transitions, these couplings are not related by $SU(3)$ symmetry; thus there is no phase prediction without referring to higher, more uncertain symmetry schemes. The phases have been measured by the ACCMOR Collaboration [11] for charged π_2 decay in the diffractive reaction $\pi^- p \to \pi^-\pi^-\pi^+ p$ to be small. However, large corrections due to interference with non-resonant "Deck"-type background had to be introduced in this analysis. Furthermore, in the final state $\pi^+\pi^-\pi^0$ studied here the interference pattern is completely different so that a simple application of their results is questionable.

For the analysis of different resonances and resonance models, we have generated Monte Carlo events for invariant $\gamma\gamma$ masses between 0.7 and 3 GeV with a $\gamma\gamma \to \pi^+\pi^-\pi^0$ matrix element constant in $W_{\gamma\gamma}$. The dependence on the virtual photons' invariant mass squared $-Q_i^2$, $i=1,2$ is taken to follow a ρ pole, as expected from vector meson dominance. For the connection of the $\gamma\gamma$ cross section (4) and the actually measurable $e^+e^- \to e^+e^-3\pi$ cross section we use the exact QED

* Note that (2) will give different values for helicities $\lambda = +2$ and -2, if any interference is occuring (e.g. between ρ^+ and ρ^-) [28]. However, after squaring and integrating over either Dalitz plot or decay plane angular variables this effect vanishes, thus there is no difference of the Dalitz plot or the angular distributions of the decay plane orientation. In this article $\lambda=2$ refers to both helicity states. The difference shows up only in correlations between Dalitz plot and angular variables which we do not use in this analysis

formulae as given by Budnev et al. [17]. The contribution of longitudinal photons to the cross section vanishes at $Q_i^2 \to 0$ due to gauge invariance [20]. It can be neglected in the kinematical region of this experiment, in which the Q_i^2 are limited to small values through anti-tag and $p_\perp$ cut requirements. The decay of the $\gamma\gamma$ system into $\pi^+\pi^-\pi^0$ is simulated according to isotropic phase space.

The events are passed through a detailed detector simulation program. Event reconstruction and selection then proceed as for real data, starting from simulated wire hits and deposited energies in the calorimeter and continuing with trigger and filter simulation. Resonance parameters such as mass and width, radiative width and helicity ratio are then determined by weighting the Monte Carlo events with the sum of squared matrix elements according to the resonance models described above, so as to obtain optimal agreement between the experimental spectra and the corresponding Monte Carlo expectation. A more detailed description of the formulae and procedures applied in the analysis can be found elsewhere [31].

5 Analysis of $\gamma\gamma \to a_2$

To enhance the relative a_2 resonance contribution we take advantage of the fact that the 3π decay of the a_2 proceeds entirely through intermediate charged ρ's [12]. At least one of the $\pi^\pm\pi^0$ mass combinations is therefore required to lie between 550 and 900 MeV. Furthermore, due to the constructive interference between the two ρ charge states (see above) one expects a large enhancement in the ρ band overlap region. An efficient selection criterion is thus provided by the distance r_ρ from the actual Dalitz (i.e. $m^2_{\pi^+\pi^0} - m^2_{\pi^-\pi^0}$ correlation) plot position to the nominal $m^2_{\rho^+} - m^2_{\rho^-}$ crossing point. For the following plots we use $r_\rho < 0.32$ GeV^2. The 3π-mass spectra of the 1γ and the 2γ samples obtained after these cuts are shown in Fig. 4. We fit the mass spectra to the a_2 Monte Carlo expectation (with mass and width fixed to the nominal PDG-values) plus a smooth background, whose shape is taken from Monte Carlo events with a $\gamma\gamma \to \pi^+\pi^-\pi^0$ matrix element constant in $W_{\gamma\gamma}$ and with phase space angular distributions. The fit therefore has two free parameters, namely the normalisations of the resonance and of the background contributions. Using helicity 2 angular distributions for the a_2 decay (as justified below), the resulting number of candidates (335 ± 30 1γ and 80 ± 11 2γ) can be converted into the following values for the radiative width:

$$1\gamma \text{ sample: } \Gamma_{\gamma\gamma}^{(\lambda=2)} = 0.99 \pm 0.09 \text{ (stat.) keV} \quad (7)$$

$$2\gamma \text{ sample: } \Gamma_{\gamma\gamma}^{(\lambda=2)} = 1.00 \pm 0.14 \text{ (stat.) keV.} \quad (8)$$

Excellent agreement is observed between the results of the two different samples, giving confidence in the photon simulation systematics. We therefore can combine the two results to reduce the statistical error:

$$\Gamma_{\gamma\gamma} = 1.00 \pm 0.07 \text{ (stat.)} \pm 0.15 \text{ (syst.) keV.} \quad (9)$$

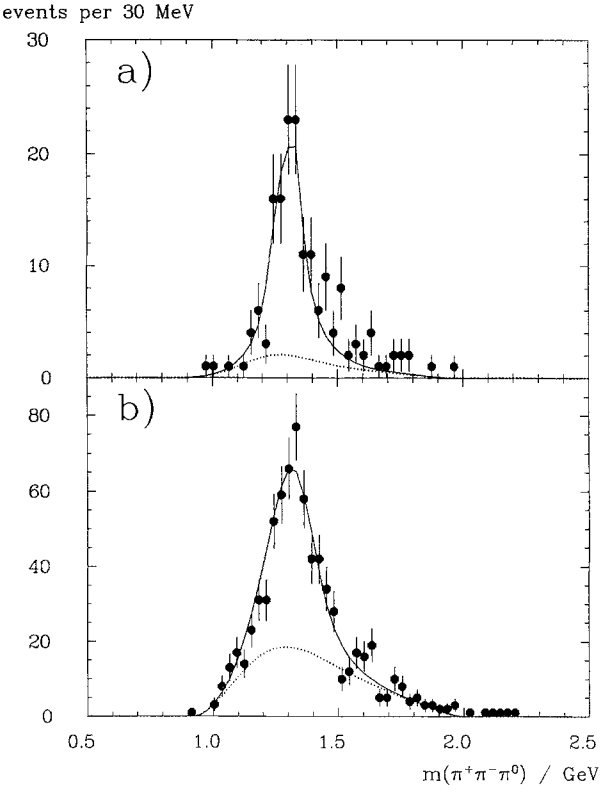

Fig. 4. Invariant $\pi^+\pi^-\pi^0$ mass after a_2 selection **a** 2γ sample, **b** 1γ sample

This result is found to be stable, within the statistical error, against drastic changes of cut values, in particular the r_ρ cut. The systematic error has been estimated through quadratic addition of the following contributions: uncertainty in luminosity (3%), effect of Q^2 evolution of form factors (3%), uncertainties in trigger simulation (5%), photon (8%) and track (4%) reconstruction efficiencies, background parametrisation (8%) and the a_2 branching ratio (4%), amounting to a total of 15%.

Owing to differing acceptances the value for the radiative width strongly depends on the helicity assumption: using helicity 0 angular distributions in the Monte Carlo simulation we would give a radiative width only about half of that quoted above. From theory (see below) one expects that the tensor meson coupling to two real photons is dominated (to varying degrees) by the helicity 2 amplitude, and some measurements indicate this behaviour [4, 5, 8], however with large uncertainties. Thus, to get a model independent value for the radiative width as well as to achieve some insight into the dynamics we have determined the helicity structure of the a_2 formation from the present data.

The complete information available for such an analysis is the correlation of the three Euler angles which describe the rotation of the $\gamma\gamma$ helicity system to the decay (Dalitz plot) system in the $\gamma\gamma$ c.m.s. However, the azimuthal angle α describing a rotation around the $\gamma\gamma$ axis cannot be measured in an untagged $\gamma\gamma$ experiment and thus has to be integrated over. We therefore analyse the correlation between $\cos\beta$ and γ, β being the polar angle between the decay plane normal and the incoming

photon radiated off the electron γ_{e^-}, and γ denoting the angle between the π^0 and the incoming γ_{e^-} projected onto the decay plane.

The expected correlation plots for a_2 decays in the helicity 2 and 0 states as well as phase space angular distributions after the complete Monte Carlo chain are shown in Fig. 5, along with the real data with invariant masses between 1.17 and 1.49 GeV, both 1γ and 2γ samples added. It is clearly evident that the data are much better described by helicity 2 than 0. To achieve a quantitative statement, we have performed a maximum likelihood fit using $\Gamma_{\gamma\gamma}$, the relative helicity 2 contribution $R^{(2)}=\Gamma_{\gamma\gamma}^{(\lambda=2)}/\Gamma_{\gamma\gamma}$ and the number of background events N_{bg} as free parameters, assuming Poisson statistics in 20 bins on the $\cos\beta-\gamma$ correlation plot. The angular distributions of the background events are modelled according to isotropic phase space. The likelihood function employed also contains a term taking into account the deviation of the background level from the expectation of the fit to the mass spectrum. The fits were carried out separately on the 1γ and 2γ samples. Both give consistent results, the combined result being:

$$R^{(2)}=\frac{\Gamma_{\gamma\gamma}^{(2)}}{\Gamma_{\gamma\gamma}}=1.04\pm0.05. \tag{10}$$

Lying above unity, this results is consistent with no helicity 0 contribution. To obtain an upper limit for the helicity 0 contribution, we follow the procedure proposed by the Particle Data Group [12] and plot the probability density, i.e. the likelihood function without taking the logarithm, as a function of the ratio $R^{(2)}$, at each point maximizing with respect to the other free parameters. In particular, to become more independent of the assumption on the background angular distributions we allow it to be an arbitrary mixture of phase space and the spin 2 – helicity 2 model. Since this flattens the likelihood function as a function of $R^{(2)}$, it results in a conservative upper limit taking into account the background model uncertainty. We then multiply the curves from the two data samples, and normalise the area under the resulting curve in the physical region to 1. The 95% confidence level limit is then obtained by determining the $R^{(2)}$ value which separates the leftmost 5% of the area in the physical region. The result is:

$$R^{(2)}>91.8\% \text{ (at 95\% c.l.)}. \tag{11}$$

This is the most stringent experimental limit yet for helicity 2 dominance in $\gamma\gamma\to a_2$ formation, to be compared with the values 0.62 ± 0.39 (PLUTO [4]), 1.00 ± 0.10 (Crystal Ball [5]) and 0.987 ± 0.083 (TPC [8]). Assuming Gaussian errors (which in our case is a good approximation near the maximum), we combine these measurements and obtain $R^{(2)}=1.018\pm0.039$. The 95% c.l. lower limit inferred from the combined likelihood function is increased to 92.7%. Since the derivation of limits in the case of unphysical best fits is not unique and not undebated (see [12]), we also quote a limit derived in the most conservative way, i.e. 95% c.l. limit is equal to the border of physical region $\pm1.96\sigma$(fit). Thus, using the combined data, it is safe to say that the helicity 0 fraction is lower than 7.7%:

$$R^{(0)}<0.077 \text{ at 95\% c.l.} \tag{12}$$

This stringent limit for the first time makes it possible to distinguish between different dynamical models for the coupling of a tensor meson to two real photons. The lowest order gauge invariant and Bose symmetric Born term amplitude predicts a helicity ratio $\Gamma_{\gamma\gamma}^{(2)}/\Gamma_{\gamma\gamma}^{(0)}=6:1$, i.e. $R^{(2)}=1/7=14.3\%$ [16]. Models in which the transition occurs in analogy to hadronic couplings (VDM) with $L=0$ dominance or electromagnetic couplings with $E1$ dominance [32], as well as static quark model pictures (relating the $\gamma\gamma$ coupling to dipole moments) [20] lead to the same helicity 0 contribution. Such a value is now excluded at a level of more than 3.5 standard deviations. The present measurement thus argues in favour of the following approaches: Nonrelativistic quark model [33] ($R^{(0)}=0$), relativistic $q\bar{q}$ bound state calculation using the Bethe-Salpeter equation [34] ($R^{(0)}$ negligible), VDM extended by describing the tensor meson coupling in analogy to the electromagnetic field tensor [35] ($R^{(0)}=0$), and the Grassberger-Kögerler sum rule [36] ($R^{(0)}\ll 1/7$).

Quark model predictions and some experimental evidence suggest that there might exist mass degenerate scalar mesons associated to each tensor meson. Due to the absence of one azimuthal angle it is then possible to confuse helicity 2 with a coherent sum of spin 0 and spin 2, helicity 0, such that helicity ratios determined without the allowance of interference have to be interpreted with care. Note, however, that this complication does not occur in the $\rho\pi$ final state analysed here, because its coupling to a scalar state is forbidden by parity.

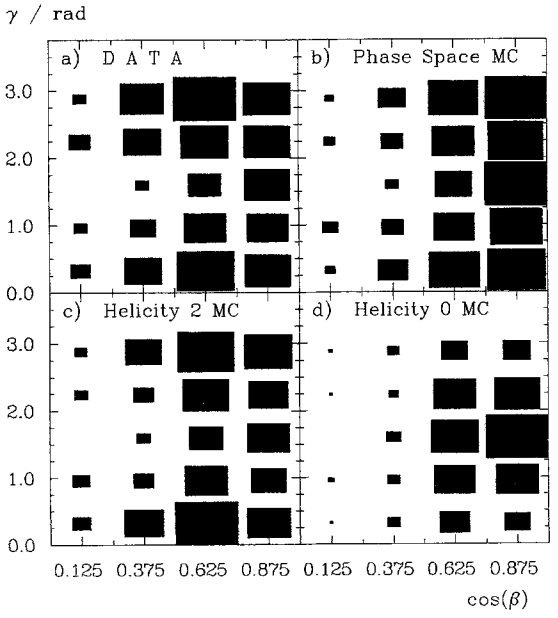

Fig. 5a–d. Correlation plots of the Euler angles γ vs. $|\cos\beta|$, **a** data, **b** Monte Carlo phase space, **c** a_2 Monte Carlo, helicity 2, **d** a_2 Monte Carlo, helicity 0

Instead, the suppression of the helicity 0 amplitude of the a_2 established here has been used [37] to set a limit on the $\gamma\gamma$ width of the narrow scalar $a_0(1300)$ recently announced by GAMS [38]: The analysis of the published [5] Crystal Ball angular distribution of the reaction $\gamma\gamma \to \eta\pi$ in the a_2 region leads to the limit $\Gamma_{\gamma\gamma}(a_0(1300)) \cdot B(a_0(1300) \to \eta\pi) < 0.44$ keV.

6 Analysis of $\gamma\gamma \to \pi_2$

The main decay mode of the $\pi_2(1670)$ is $f_2(1270)\,\pi^0$ with a branching ratio of $53 \pm 5\%$. The most promising way to identify such a broad resonance in a reaction dominated by $\rho^\pm \pi^\mp$ is thus to search for f_2 production in the invariant $\pi^+\pi^-$ mass spectrum. The initial event selection is as in section 3. To enhance the relative contribution of a $J^P = 2^- \to 0^- 2^+$; $2^+ \to 0^- 0^-$ decay chain, we demand $|\cos\theta_{\pi^+}| < 0.45$, where θ_{π^+} denotes the polar angle of the positive pion in the f_2 c.m.s. with respect to the $\gamma\gamma$ (i.e. $z-$) axis. This cut is motivated by the expected $|Y_2^0|^2 \propto (3\cos^2\theta - 1)^2$ behaviour of this angular distribution together with a small acceptance beyond the zero of this distribution. We furthermore only accept events with a small angle between decay plane normal and $\gamma\gamma$ axis: $|\cos\beta| > 0.7$.

The invariant $\pi^+\pi^-$ mass spectrum of the remaining 413 1γ and 75 2γ events with 3π masses between 1.45 and 2.05 GeV is shown in Fig. 6. We observe clear evidence for $f_2(1270)$ production. The lines show the results of 2 parameter fits of a $\pi_2 \to f_2\,\pi^0$ decay model with standard resonance parameters plus a background whose shape is taken from phase space Monte Carlo plus the remaining absolutely normalised a_2 background (shaded). The different lines are for different interference patterns between the main decay modes (see below).

To investigate the W-dependence of the f_2 production we perform a number of such fits in overlapping bins of 250 MeV width. The resulting f_2 candidate spectrum is shown in Fig. 7a. Note that only every fifth bin is statistically independent. A Monte Carlo calculation of π_2 formation and decay using the standard PDG mass and width and neglecting other 3π decay modes and interference with them leads to the solid line, the normalisation of which is obtained by a fit to the data. We interpret the resonance like structure in this plot, as well as the agreement with expectations, as clear evidence for exclusive π_2 production.

To determine the mass and width of the resonance, we have performed a least squares fit of the excitation

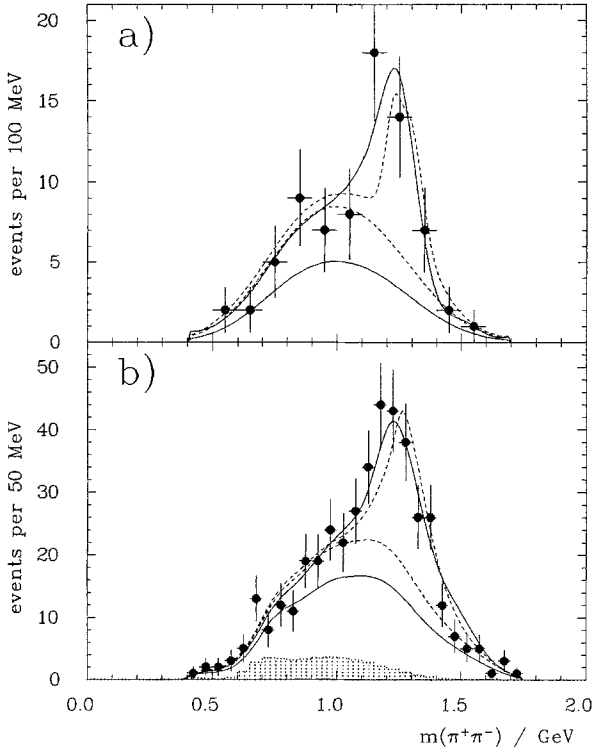

Fig. 6a, b. Invariant $\pi^+\pi^-$ mass for events with 3π mass between 1.45 and 2 GeV, after π_2 selection. **a** 2γ sample, **b** 1γ sample. The lines are results of fits of a π_2 decay model with constructive (solid) and destructive (dashed) interference between the $f_2\,\pi^0$ and $\rho\pi$ decay modes, and a background which is composed from a_2 (fixed normalisation) and a shape suggested by phase space Monte Carlo

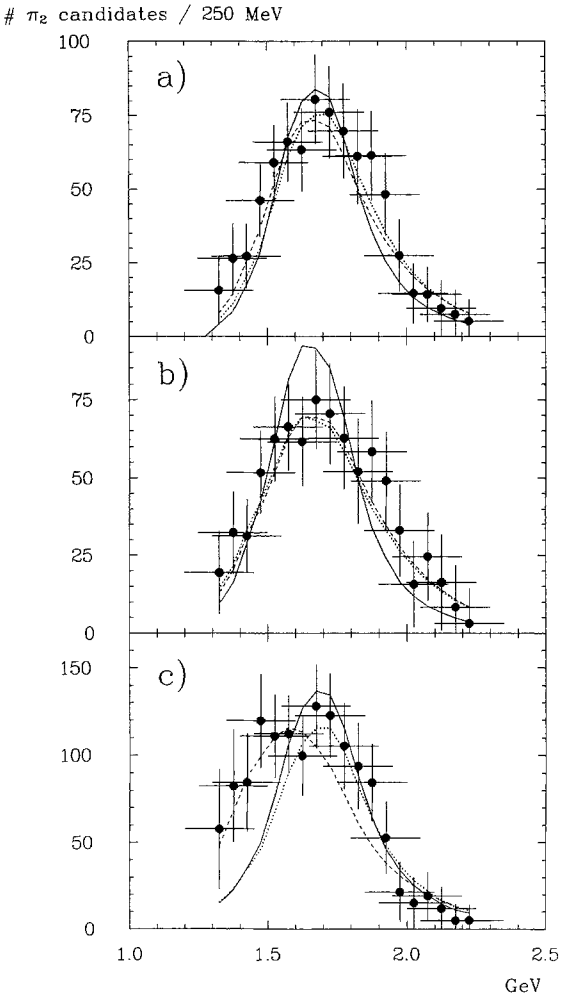

Fig. 7a–c. Number of $\pi_2(1670)$ candidates as a function of the 3π mass (2γ and 1γ samples added) using different π_2 decay models. The solid line is the Monte Carlo expectation using standard PDG values for the π_2, dotted: PDG mass, width free, dashed: mass and width free. **a** incoherent $f_2\,\pi^0$ decay mode, **b** coherent addition of $f_2\,\pi^0$ and $\rho\pi$, **c** coherent subtraction of $f_2\,\pi^0$ and $\rho\pi$

curve to a single relativistic Breit-Wigner, taking into account the correlation between the bins. Photon flux, acceptance, detector resolution and binning effects are fully unfolded. This is achieved by recalculating the Monte Carlo expectation histogram in each iteration by looping over all Monte Carlo events. When filling the histogram, each event is weighted by the factor $\sigma_{\gamma\gamma}^{\text{fit}}/\sigma_{\gamma\gamma}^{\text{MC}}$, where $\sigma_{\gamma\gamma}^{\text{fit}}$ denotes the resonance cross section of (4) depending on the fit parameters m_{π_2}, Γ_{π_2}, $\Gamma_{\gamma\gamma}$ and $\sigma_{\gamma\gamma}^{\text{MC}}$ represents the (flat) cross section used in the Monte Carlo generation. The result is $m=1.610\pm0.094$ GeV and $\Gamma=0.420\pm0.230$ GeV, well compatible with the standard values [12] within the large errors.

Apart from the $f_2\pi^0$ decay mode, two other 3π decay modes have been observed [12]: $\rho\pi$ with a branching ratio of $34\pm6\%$ and $\pi(\pi\pi)_{s\text{-wave}}$ with $9\pm5\%$. In the following we neglect the effect of a possible $\pi(\pi\pi)_{s\text{-wave}}$, because the contribution is small and only of marginal significance (1.8σ). We further do not take into account the possible D-wave admixture [11] in the $f_2\pi$ decay mode.

A Monte Carlo study shows that interference between the $f_2\pi^0$ and $\rho^{\pm}\pi^{\mp}$ decay modes in the final state $\pi^+\pi^-\pi^0$ is substantial and leads, depending on the relative phase, to very different $\pi^+\pi^-$ mass spectra. This is in marked contrast to the $3\pi^0$ decay mode observed by the Crystal Ball Collaboration [9], where no $\rho\pi$ contribution appears and interference between the 3 possible f_2 combinations occurs only outside the nominal Dalitz plot boundaries. As an example, we show in Fig. 8 the Monte Carlo predictions for the observed $\pi^+\pi^-$ mass spectrum for $f_2\pi+\rho\pi$ and $f_2\pi-\rho\pi$ using the coupling constants derived from the branching ratios. It becomes clear that, unless more about the relative phase is known, the radiative width is not well determined from the data, because of the completely different shape and normalisation. Using these two extreme models, we perform fits

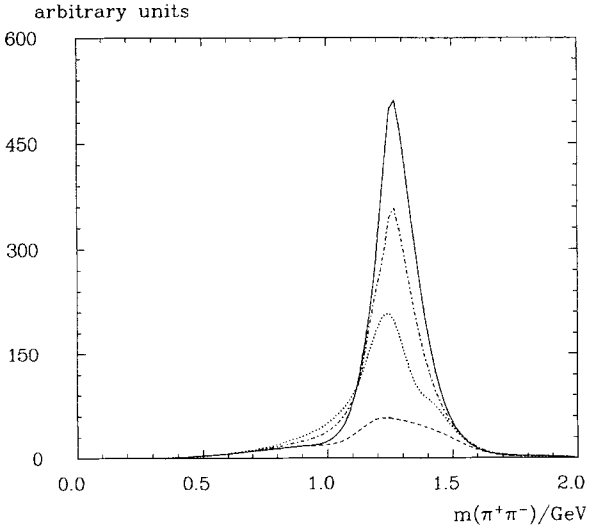

Fig. 8. Monte Carlo expectation for the invariant $\pi^+\pi^-$ mass spectrum considering $f_2\pi$ and $\rho\pi$ decay modes of the π_2 using standard PDG branching ratios. Solid line: coherent addition; dotted line: coherent subtraction; dashed line: $\rho\pi$ part only; dash-dotted line: incoherent addition

analogous to the incoherent case described above. We arrive at the values:

incoherent ansatz:
$$\Gamma_{\gamma\gamma}(\pi_2(1670))=1.3\pm0.3\,(\text{stat.})\ \text{keV} \tag{13}$$

coherent addition:
$$\Gamma_{\gamma\gamma}(\pi_2(1670))=0.8\pm0.3\,(\text{stat.})\ \text{keV} \tag{14}$$

coherent subtraction (mass fixed):
$$\Gamma_{\gamma\gamma}(\pi_2(1670))=1.5\pm0.5\,(\text{stat.})\ \text{keV}. \tag{15}$$

The corresponding W-dependence plots are shown in Fig. 7b and c. In the case of constructive interference the fitted mass is 1.684 ± 0.082 GeV in excellent agreement with the nominal value.

As already mentioned, the ACCMOR data [11] indicate a relative phase close to zero (constructive interference). In order to get some information from our data, we investigated the Monte Carlo predictions with various phases and compared kinematical distributions to the data.

The first suggestion against destructive interference comes from the W dependence Fig. 7c. The central mass fitted to this spectrum is $m=1.495\pm0.085$ and thus 2 standard deviations off the nominal value [12].

The neutral $\pi\pi$ mass combinations can be described by all three models (c.f. Fig. 6). The slight downward shift of the f_2 peak position may be explained by the presence of a D-wave contribution. Also the gross features of the charged $\pi\pi$ mass spectra can be reproduced, though not all the details. A fit to the $m(\pi^{\pm}\pi^0)$ vs. $m(\pi^+\pi^-)$-correlation plot (with two entries per event) to a simple resonance+phase space+fixed a_2 background model prefers the constructive interference model against the incoherent ($\Delta\log L=1.8$) and the destructive interference ($\Delta\log L=8.5$). It thus seems that the latter possibility can be ruled out.

We thus consider the number obtained using the constructive coherent model (see Fig. 7b)) as our final result:

$$\Gamma_{\gamma\gamma}(\pi_2(1670))=0.8\pm0.3\,(\text{stat.})\pm0.12\,(\text{syst.})\ \text{keV} \tag{16}$$

$$m(\pi_2(1670))=1.684\pm0.082\ \text{GeV} \tag{17}$$

$$\Gamma(\pi_2(1670))=0.54\pm0.32\ \text{GeV} \tag{18}$$

assuming the validity of the PDG branching ratios and constructive interference between the $f_2\pi$ and $\rho\pi$ isobars. The contributions to the given systematic error given is analogous to the a_2. Note however, that the strong dependence on the interference assumptions is not included. All other phase assumptions will lead to larger $\gamma\gamma$ widths; the incoherent ansatz leading to $1.3\pm0.3\pm0.2$ keV.

7 Summary and conclusions

We have performed an analysis of the reaction $\gamma\gamma\to\pi^+\pi^-\pi^0$ in the no tag mode using $86\,\text{pb}^{-1}$ of data taken with the CELLO detector at PETRA with a beam energy of 17.5 GeV. To increase statistics and to be less

sensitive to photon detection systematics we have analysed two samples, one with the π^0 fully reconstructed and one with only one photon detected. Throughout, the two analyses give consistent results. We observe clear evidence for the formation of the tensor meson $a_2(1320)$ and the pseudo tensor meson $\pi_2(1670)$. The measured radiative width of the a_2 is $\Gamma_{\gamma\gamma}(a_2) = 1.00 \pm 0.07$ (stat.) ± 0.15 (syst.) keV. An angular correlation analysis shows that helicity 0 does not contribute to the $a_2 - \gamma\gamma$ coupling, resulting in an upper limit of $R^{(0)} = \Gamma_{\gamma\gamma}^{(\lambda=0)}/\Gamma_{\gamma\gamma} < 8.2\%$ (at 95% c.l.), which is improved by combination with previous measurements to 7.7%. This tight upper limit for the first time excludes some dynamical models, e.g. the prediction $R^{(0)} = 1/7$ from the lowest dimensional Born term.

π_2 resonance formation is established through the identification of the $f_2\pi^0$ mode. The measured mass and width are $m = 1.684 \pm 0.082$ GeV and $\Gamma = 0.54 \pm 0.32$ GeV. It is shown that the determination of the π_2 radiative width from the $f_2\pi^0$ invariant mass curve is strongly dependent on the degree of coherence and the relative phases between different isobars. If interference is neglected, the radiative width of the π_2 is determined as $\Gamma_{\gamma\gamma}(\pi_2(1670)) = 1.3 \pm 0.3 \pm 0.2$ keV. Destructive interference between the $f_2\pi^0$ and $\rho\pi$ decay modes is ruled out. Constructive interference leads to the substantially smaller value of $\Gamma_{\gamma\gamma}(\pi_2(1670)) = 0.8 \pm 0.3 \pm 0.12$ keV.

Acknowledgements. We greatfully acknowledge the outstanding efforts of the PETRA machine group which made possible these measurements. We are indebted to the DESY computer centre for their excellent support during the experiment. We acknowledge the invaluable effort of the many engineers and technicians from the collaborating institutions in the construction and maintainance of the apparatus, in particular the operation of the magnet system by M. Clausen, P. Röpnack and the cryogenic group. The visiting groups wish to thank the DESY Directorate for the support and kind hospitality extended to them. This work was partly supported by the Bundesministerium für Forschung und Technologie (Germany), by the Commissariat à l'Energie Atomique and the Institut National de Physique Nucléaire et de Physique des Particules (France), by the Instituto Nazionale di Fisica Nucleare (Italy), by the Science and Engineering Research Council (UK) and by the Ministry of Science and Development (Israel).

References

1. Crystal Ball Coll. (at SPEAR), C. Edwards et al.: Phys. Lett. 110 B (1982) 82
2. JADE Coll. (preliminary), see J.E. Olsson: Procs. V.th Int. Workshop on Photon-Photon Collisions, Aachen 1983, Springer
3. CELLO Coll. H.J. Behrend et al.: Phys. Lett. 114 B (1982) 378; Erratum Phys. Lett. 125 B (1983) 518
4. PLUTO Coll. Ch. Berger et al.: Phys. Lett. 149 B (1984) 427
5. Crystal Ball Coll. (at DORIS) D. Antreasyan et al.: Phys. Rev. D 33 (1986) 1847
6. TASSO Coll. M. Althoff et al.: Z. Phys. C – Particles and Fields 31 (1986) 537
7. JADE Coll. (preliminary), see J.E. Olsson, VIII.th Int. Workshop on Photon-Photon Collisions, Shoresh (Israel) 1988, p. 77. Singapore: World Scientific
8. A.R. Barker TPC/2γ Coll.: Ph.D. Thesis, University of California Santa Barbara, Dec. 1988
9. B. Muryn Crystal Ball Coll.: First observation of $\pi_2(1680)$ in $\gamma\gamma$ collisions, Procs. VIII. International Workshop on Photon-Photon Collisions, Shoresh (Israel) 1988, p. 102. Singapore: World Scientific
10. Crystal Ball Coll., see J.K. Bienlein: Procs. BNL Workshop on Glueballs, Hybrids and Exotic Hadrons, Upton, New York 1988, p. 486. New York: AIP 1989
11. ACCMOR Coll. C. Daum et al.: Nucl. Phys. B 182 (1981) 269
12. Particle Data Group: Phys. Lett. B 204 (1988) 1–486
13. CELLO Coll. H.J. Behrend et al.: Phys. Scr. 23 (1981) 610
14. H.J. Behrend: Comput. Phys. Commun. 22 (1981) 365
15. M. Feindt: $\gamma\gamma$ Exclusive, PLUTO' last and CELLO's latest. Procs. VIII. International Workshop on Photon-Photon Collisions, Shoresh (Israel) 1988, p. 3. Singapore: World Scientific
16. M. Feindt: The partial wave analysis formalism for $\gamma\gamma$ interactions in e^+e^- reactions. DESY report, in preparation
17. V.M. Budnev, I.F. Ginzburg, G.V. Meledin, V.G. Serbo: Phys. Rep. 15 C (1975) 181
18. L. Landau: Dokl. Akad. Nauk. SSSR 60 (1948) 207
19. C.N. Yang: Phys. Rev. 77 (1950) 242
20. M. Poppe: Int. J. Mod. Phys. 1 (1986) 545
21. C. Zemach: Phys. Rev. 133 B (1964) 1201; Phys. Rev. 140 B (1965) 97; Phys. Rev. 140 B (1965) 109
22. W.R. Frazer, J.R. Fulco, F.R. Halpern: Phys. Rev. 136 (1964) B 1207
23. R.J. Cashmore: Amplitude analysis in three body final states. Procs. 14th Scottish Universities Summer School in Physics, 1973. New York: Academic Press 1974
24. Three particle phase shift analysis and meson resonance production. Daresbury Study Weekend Series No. 8, 1975, ed. J.B. Dainton and A.J.G. Hey.
25. D. Aston, T.A. Lasinski, P.K. Sinervo: The SLAC three-body partial wave analysis system, SLAC-287, 1985
26. PLUTO Coll. Ch. Berger et al.: Z. Phys. C – Particles and Fields 37 (1988) 329
27. M. Feindt: Ph.D. Thesis, DESY-F14-88/02 (1988)
28. B. Boštjančič ARGUS Coll.: private communication
29. J.M. Blatt, V. Weisskopf: Theoretical nuclear physics. New York: John Wiley 1952
30. H. Pilkuhn, in: Landolt-Börnstein, New Ser. Vol 6. Berlin, Heidelberg, New York: Springer 1972
31. J.H. Köhne: Diploma Thesis, University of Hamburg, Internal Report DESY-FCE-89-03 (1989)
32. W.N. Cottingham, I.H. Dunbar: J. Phys. G 5 (1979) L155
33. H. Krasemann, J. Vermaseren: Nucl. Phys. B 184 (1981) 269
34. L. Bergström, G. Hulth, H. Snellman, Z. Phys. C – Particles and Fields 16 (1983) 253
35. N.N. Achasov, V.A. Karnakov: Novosibirsk TF 14-147 (1985)
36. P. Grassberger, P. Kögerler: Nucl. Phys. 106 B (1976) 451
37. M. Feindt: Light Hadrons as Seen via Two Photons in CELLO, DESY-89-142, to be published in Procs. III. Int. Conference on Hadron Spectroscopy, Ajaccio (France) 1989, éditions Frontières
38. GAMS-NA12 Coll., see M. Boutemeur: Procs. BNL Workshop on Glueballs, Hybrids and Exotic Hadrons, Upton, New York 1988, p. 389; New York: AIP 1989; M. Boutemeur: Procs. III. Int. Conference on Hadron Spectroscopy, Ajaccio (France) 1989, éditions Frontières